Deficiency of adenosine deaminase 2 skews adaptive immune repertoires toward specific sets of T- and B-cell receptors

Christoph Schultheiß, PhD,[a,b]* Paul Schmidt-Barbo, MSc,[a,b,c]* Lisa Paschold, PhD,[d] Carl Esperanzate, BSc,[e] Alissa Behn, MSc,[d] Rafael Mikolajczyk, MD, MSc,[f] Daniel L. Kastner, MD, PhD,[e] Ivona Aksentijevich, MD,[e] and Mascha Binder, MD[a,b,c] *Basel, Switzerland; Freiburg and Halle, Germany; and Bethesda, Md*

Background: Adenosine deaminase 2 deficiency (DADA2) is a genetic disorder caused by biallelic hypomorphic or loss-of-function mutations in the *ADA2* gene, which encodes a protein deaminase regulating extracellular adenosine metabolism. Clinical features encompass inflammatory vasculopathy, early-onset strokes, and a complex presentation involving both immunodeficiency and autoinflammation/autoimmunity.
Objective: Our aim was to determine a DADA2-specific adaptive immune architecture.
Methods: We profiled immunoglobulin levels and peripheral B- and T-cell phenotypes in 47 previously reported and 5 unreported patients with DADA2. Levels of 21 cytokines and chemokines were quantified in patients with or without anti-TNF treatment. To characterize the DADA2 immune architecture, we performed T- and B-cell receptor immunosequencing. We trained a binary LightGBM classifier to distinguish DADA2 T- and B-cell immune repertoires from healthy individuals.
Results: We detected hypogammaglobulinemia in 65% of patients with DADA2 (34 of 52) and cytopenias in 48% (25 of 52). Flow cytometric profiling revealed contraction of B- and T-cell memory compartments. In addition, we observed elevated levels of TNF, IL-8, several interferons, a proliferation-inducing ligand (APRIL), B-cell activating factor (BAFF), and soluble CD40 ligand (sCD40L). High serum levels of TNF, BAFF, and sCD40L persisted under anti-TNF therapy. Next-generation immunosequencing of peripheral lymphocytes showed restricted T-cell receptor repertoires and B cells, which were particularly skewed toward immunoglobulin heavy chain V4-34 rearrangements. With high accuracy, our machine learning algorithm separated individuals with DADA2 from healthy individuals on the basis of immunogenetic parameters regarding B-cell clone fraction, CDR3 length, and selected Kidera factors.
Conclusions: Our findings underscore the significant influence of ADA2 on the adaptive immune system, which results in a highly specific immunogenetic signature in patients with DADA2. (J Allergy Clin Immunol 2025;155:1664-74.)

Key words: *DADA2, immune repertoire, BCR, TCR, immune architecture, autoimmunity, machine learning, TNF*

Along with their cognate adenosine or nucleotide receptors, adenosine and related purine nucleosides constitute a multifaceted and highly plastic cell-to-cell communication system that is operating across tissues and species.[1-3] Adenosine deaminase 2 (ADA2) is considered to catalyze the deamination of extracellular adenosine to inosine and represents an important module within this regulatory network.[4,5] However, it was also recently described as a lysosomal DNA-editing enzyme in the context of Toll-like receptor–mediated DNA sensing.[6] Biallelic hypomorphic or loss-of-function germline mutations in the *ADA2* (*CECR1*) gene cause deficiency of adenosine deaminase 2 (DADA2), a rare autoinflammatory condition hallmarked by vasculitis of medium and small vessels mimicking polyarteritis nodosa and heterogenous inflammatory manifestations, including recurrent fever, livedo reticularis, and subcortical (lacunar) ischemic strokes.[7-11] Patients with complete enzyme deficiency present with bone marrow failure[12] and are often diagnosed with pure red aplasia or Blackfan-Diamond anemia. In contrast to its intracellular isoenzyme adenosine deaminase 1 (ADA1 or ADA), ADA2 is a secreted protein and expressed mainly by myeloid cells.[4] The involvement of ADA2 in extracellular adenosine catabolism may explain its relevance for adaptive immunity that is clinically reflected by the mild immunodeficiency and autoimmunity phenotype observed in many patients with DADA2.[13]

Only limited knowledge about the adaptive immune fingerprint in patients with DADA2 exists. Most patients have normal T-cell counts, but a T follicular helper cell defect or $CD4^+$ T-cell lymphopenia has been suggested to contribute to impaired B-cell help.[14] Patients show a significant decrease in memory B cells, in particular, class switch memory, as well as expansion of $CD21^{low}$ B cells that are recognized for their role in autoimmune diseases.[15] Interestingly, patients with DADA2 may have variable absolute B-cell numbers ranging from B lymphopenia to high B-cell counts. Hypogammaglobulinemia, with low levels of IgM, IgG, and/or IgA, is a frequent finding that often necessitates immunoglobulin substitution, and low serum immunoglobulin levels may correlate with inflammatory disease activity.[13]

From [a]the Division of Medical Oncology, University Hospital Basel; [b]the Laboratory of Translational Immuno-Oncology, Department of Biomedicine, University and University Hospital Basel; Basel; [c]the Collaborative Research Institute Intelligent Oncology (CRIION), Freiburg; [d]the Internal Medicine IV, Oncology/Hematology, and [f]the Institute for Medical Epidemiology, Biometrics and Informatics, Interdisciplinary Centre for Health Sciences, Medical Faculty, Martin-Luther-University Halle-Wittenberg; and [e]the Inflammatory Disease Section, National Human Genome Research Institute, National Institutes of Health, Bethesda.

*These authors contributed equally to this work.

Received for publication October 8, 2024; revised January 20, 2025; accepted for publication January 29, 2025.

Available online February 7, 2025.

Corresponding author: Mascha Binder, MD, Medical Oncology, University Hospital Basel, Petersgraben 4, Basel 4031 Switzerland. E-mail: Mascha.Binder@usb.ch.

0091-6749

https://doi.org/10.1016/j.jaci.2025.01.032

Abbreviations used
ADA: Adenosine deaminase
APRIL: A proliferation-inducing ligand
BAFF: B-cell activating factor
BCR: B-cell receptor
CDR3: Complementarity determining region 3
DADA2: Deficiency of adenosine deaminase 2
HA20: Haploinsufficiency of A20
IGH: Immunoglobulin heavy chain
LightGBM: Light gradient boosting machine
NF-κB: Nuclear factor-κB
NIH: National Institutes of Health
PC: Principal component
PCA: Principal component analysis
sCD40L: Soluble CD40 ligand
TCR: T-cell receptor
TRB: T-cell receptor β-chain

In line with this, low vaccine responses have been noted in a percentage of cases.

In addition to a higher infection susceptibility, autoimmune disease resembling SLE and autoimmune cytopenia has been reported in several families.[16,17] Lymphoproliferative disease with generalized lymphadenopathy is seen in more than 10% of affected individuals, with splenomegaly being common (including in a few individuals with childhood-onset Hodgkin lymphoma).[18]

Here, we used a cohort of 52 patients with DADA2 to systematically study adaptive immunity. Our immunogenetic analyses reveal an imprint of T- and B-cell repertoires mediated by the *ADA2* deficiency that is likely driven by the deregulated myeloid-derived cytokines in these patients. This imprint not only reflects clinical autoimmunity but may also explain the propensity for lymphomas in patients with DADA2.

METHODS

The DADA2 and control cohorts

DADA2 was a real-life cohort from National Human Genome Research Institute in Bethesda, Maryland. Patients with DADA2 were enrolled in a natural history protocol that was approved by the National Institutes of Health (NIH) institutional review board and underwent full evaluation at the NIH Clinical Center. Informed consent/assent was obtained as appropriate for all patients and parents. Blood from healthy donors was collected for scientific purposes after they had provided informed consent, as approved by the ethics commission Halle (Saale) (project no. 2014-75). PBMCs were isolated from blood by standard Ficoll gradient centrifugation. Genomic DNA was extracted from PBMCs by using the GenElute Mammalian Genomic DNA Miniprep Kit (Sigma-Aldrich, St Louis, Mo).

Flow cytometry

Quantification of serum immunoglobulin levels and profiling of B- and T-cell populations were performed during routine clinical testing, as described in Barron et al.[19] Cytokine serum levels were measured by using the LEGENDplex Human B-Cell Panel (13-plex) and the Human Anti-Virus Response Panel (13-plex) (BioLegend) according to the manufacturer's instructions. Readout was performed on a BD FACSCelesta. Data analysis was performed by using the cloud-based data analysis software suite for LEGENDplex. Cytokine correlations were calculated by using the R package corrplot.

Next-generation sequencing of T- and B-cell immune repertoires

The V(D)J rearranged immunoglobulin heavy (IGH) and T-cell receptor β-chain (TRB) loci were amplified from 250 to 500 ng of genomic DNA by using a multiplex PCR as described.[20,21] Sequencing was performed on an Illumina MiSeq (paired-end, 2 × 301 cycles, v3, chemistry), and raw reads were aligned by using the MiXCR framework.[22] As a reference for sequence alignment, the default MiXCR library was used for TRB sequences and the IMGT library, v3, for IGH. Each unique complementarity-determining region 3 (CDR3) nucleotide sequence was considered a clone. Nonproductive reads and sequences with less than 2 read counts were not considered for further bioinformatics evaluation. IGHV genes with less than 98% identity to the germline sequence were considered somatically hypermutated. All analyses and data plotting were performed by using RStudio and R version 4.2.0 and the packages tcR, ade4, and tidyverse.

Immune repertoire metrics

As a clonality index, we calculated the value *1–Pielou evenness* from T-cell receptor (TCR) and/or B-cell receptor (BCR) sequence data. Evenness measures the relative abundance of unique B- or T-cell clonotypes in the repertoire and is calculated by using the equation $J = H'/\log2(S)$, with H' being the Shannon diversity index and S being the total clone number (richness) in a distinct sample. A sample that contains only 1 clone has a clonality index of 1; complete clonal diversity is indicated by a clonality index of 0. To address sequencing depth effects, repertoires containing fewer than 10,000 reads were excluded from the final metrics analyses, and normalization was conducted to a standardized read count of 13,000 reads. The generation probability of each TRB clonotype was calculated by using the OLGA (Optimized Likelihood estimate of immunoGlobulin Amino-acid sequences) algorithm with default parameters.[23] The mean generation probability of all clonotypes per repertoire was plotted.

Data availability

The sequence data set reported herein have been deposited at the European Nucleotide Archive under the accession number PRJEB83076.

Machine learning

Data preprocessing. We collected immune repertoire data from our DADA2 cohort, as well as from our age-matched control cohort. To ensure data quality and reliability, raw sequencing reads were initially filtered to remove repertoires containing fewer than 10,000 reads. Following this, we normalized the remaining repertoires to a standardized read count of 13,000 reads to account for sequencing depth variations. Subsequently, we computed major B- and T-cell immune repertoire metrics, including clonality, Shannon diversity, richness, and the

TABLE I. Clinical characteristics of the DADA2 cohort

Patient information							Neurovascular disease		Inflammation		Vasculitis/ autoimmunity
ID	Sibling of	Sex	Age at sampling	Genotype	Treated	NGS	Stroke	No. of strokes	Fever	CRP	Livedo/skin
1		N/A	N/A	G47R/G47R	X						
2		M	12 y	R169Q /Y453C	X	X	X	8	X	X	X
4	5	M	16 y	R169Q/G47W	X	X			X	X	X
5	4	F	14 y	R169Q/G47W		X					
7		M	6 y	R169Q/W204C	X	X	X	2	X	X	
8		F	1 y	G47R/T129P	X	X				X	X
12		M	44 y	V458D/c.973-2A>G	X	X			X	X	X
13		M	14 y	G47R/P435A	X		X	3		X	X
14		F	2 y	A357T/G358R	X	X	X	2	X	X	X
15		F	14 y	Y453C/c.-47+2T>C	X	X	X	2	X	X	X
16		M	18 y	Y453C/c.-47+2T>C	X	X	X	1	X	X	X
17		F	23 y	Y453C/c.-47+2T>C	X			.			X
18		F	3 y	A109D/Y453C	X		X	4	X	X	X
19		F	1 y	G47R/G47R	X	X			X	X	X
20		F	34 y	M1T/I93T	X		X	3	X	X	X
21		M	19 y	G47A/G47A	X	X	X	11	X	X	X
22		M	25 y	G47A/R169Q	X	X	X	2		X	X
23		M	7 y	R34W/T360A		X	X	1	X	X	X
24	25	F	10 y	G47R/G358R	X	X				X	X
25	24	M	12 y	G47R/G358R	X	X	X	2	X	X	X
26		M	6 y	H112Q/del exon 7	X	X			X	X	
27	29	F	4 y	Dup.ex.7/Dup.ex.7	X	X					
29	27	F	1 y	Dup.ex.7/Dup.ex.7	X	X					
30	31	M	56 y	L188P/W501R	X	X				X	X
31	30	M	54 y	L188P/W501R	X		X	1		X	X
32		F	6 y	G47A/Y453C	X	X	X	7	X	X	X
33		F	9 y	R306X/G383S	X	X			X	X	X
34		M	23 y	H112Q/R169Q	X	X			X		
36		F	1 y	L351Q/L351Q	X		X	1	X	X	
37		F	17 y	G47A/H112Q	X	X	X	3	X	X	X
38		F	9 y	E244A/P425A	X		X	1	X	X	X
39		M	6 y	R169Q/28kb del.	X	X	X	5	X	X	X
40		F	1 y	R169Q/R169Q	X	X			X	X	X
41		F	23 y	F355L/E328K		X			X	X	X
42		M	5 y	R169Q/A357T	X				X	X	X
43		F	11 y	G47R/G47R	X	X			X	X	X
44		F	11 y	F178S/F178S	X	X			X	X	
45		F	38 y	H112Q/R34 W		X			X	X	X
46		F	19 y	R 48G/P251L	X	X	X	2	X		X
47		F	36 y	G47A/R169Q		X				X	X
48		F	1 y	G47A/c.973-2A>G	X	X	X	3			X
49		M	13 y	G47R/G47R	X	X	X	3	X	X	X
50	51	F	10 y	R312*/c.973-2A>G	X	X			X	X	X
51	50	F	14 y	R312*/c.973-2A>G	X					X	X
52		N/A	N/A	G47R/G47R	X	X					
53	Twin of 54	F	9 y	R169Q/R169Q	X	X			X		
54	Twin of 53	M	9 y	R169Q/R169Q	X	X					
55		F	17 y	N370K/c.973-2A>G	X	X	Not clear to MRI		X		X
56		M	20 y	G47V/G47V	X	X	X		X	X	
57		M	8 y	R169Q/Y453C	X	X	X	6	X	X	X
58		F	55 y	I93T/c.973-2A>G	X	X			X	X	
59		F	15 y	R169Q/N423K	X	X	X		X	X	X

Ab, Antibody; *ANA*, antinuclear antibody; *CRP*, C-reactive protein; *DBA*, Diamond-Blackfan anemia; *EM*, effector memory; *F*, female; *ID*, identifier; *Ig*, immunoglobulin; *M*, male; *MRI*, magnetic resonance imaging; *N/A*, not available; *NGS*, next-generation sequencing; *PAN*, polyarteritis nodosa.

hypermutated fraction in B-cell repertoires. Key features such as clonotype fractions, lengths of CDR3 sequences, and VDJ arrangements were extracted from each repertoire. *VDJ* genes were encoded using a one-hot encoding scheme, whereas physicochemical properties of the individual amino acid sequence of CDR3 regions were augmented by using the 10 Kidera factors.

Vasculitis/ autoimmunity			Immune dysfunction									
PAN	Raynauds	ANA	Adenopathy	Low Ig	Inadequate Ab response	Pancytopenia	Neutropenia	Thrombocytopenia	Lymphopenia	Anemia	Low $CD4^+$ EM	Low $CD20^+$ memory
					X							X
				X							X	
X		X			X		X				X	X
				X	N/A							
X				X	X							X
					X							
		X			N/A						X	X
				X	N/A						X	
X			X		X						X	
X	X			X	N/A				X		X	
X		X	X		X				X		X	X
X				X	X				X			X
		X		X								
		N/A	X	X	N/A						X	X
X				X		X						X
X	X	X		X	N/A						X	X
	X			X	N/A							
X		X		X	X					X		
X	X				X							
X	X		X									
X		X		X	X	X						X
				X	N/A							
		X		X	N/A							
X				X			X				X	X
		X		X	X				X			
X		X		X		X						
X				X						X	X	
X				X					X		X	
X				X			X				X	
X	X			X	N/A	X					X	
X												
X				X	N/A	X						
	X			X						DBA	X	X
X	X									DBA		X
			X								X	X
					X		X				X	
	X						X				X	
X											X	X
	X		X	X						X	X	X
				X	N/A							
X											X	X
	X			X			X					
		X	X	X								
					X						X	
X				X	X			X		X		X
		X		X				X				
	X		X	X		X	X	X	X		X	X
									X	X		X
				X	X	X	X	X	X	X	X	X
			N/A	X	X	X	X	X	X	X	X	X
X	X		X							X		

To address the variable number of clonotypes per repertoire, we adopted a strategy in which a fixed number n of clonotypes per repertoire was extracted on the basis of their clonotype fraction, with the remaining clonotypes discarded. For repertoires with fewer than n clonotypes, we applied zero padding to ensure consistent input dimensions across all samples. The features of

the *n* selected clonotypes and the immune repertoire metrics were concatenated into a single vector, representing each repertoire. To fully leverage both B- and T-cell information, we matched and concatenated the repertoire vectors for every subject in the study. Subjects with missing B- or T-cell repertoires were excluded from the data. Ultimately, our preprocessing pipeline resulted in matched repertoire of 22 patients with DADA2 and 37 healthy donors that was ready for further analysis.

Training. To facilitate robust model training and evaluation, we partitioned the data set into a training set comprising 75% of the data and a test set containing the remaining 25%. Importantly, we ensured that the proportions of classes were maintained in both subsets. During the training phase, we randomly traversed a predefined feature space and compared the performance of 3 distinct models: logistic regression, random forest, and light gradient boosting machine (LightGBM) classifiers. For hyperparameter tuning and model evaluation, we applied a k-fold cross-validation training regimen with *k* set to 3. To streamline model complexity and enhance interpretability, we initially reduced the feature space by excluding strongly correlated features identified within the training set. This systematic approach allowed us to fine-tune the model parameters and identify the most informative features, thereby optimizing model performance and generalization capabilities.

Testing. After thoroughly exploring the hyperparameter and feature space, we identified the best-performing models on the basis of its performance during the training phase. Subsequently, we evaluated the model's accuracy by using previously unseen test data. This evaluation step ensures that our model's performance could be assessed objectively, providing valuable insights into its effectiveness in generalization to new, unseen data. By prioritizing performance on the test set performance, we were able to ascertain a more real-world applicability and robustness. The whole analysis was implemented in python 3.11.6 with scikit-learn 1.3.2, lightgbm 4.1.0, and shap 0.45.0 by using a Conda environment (conda 24.3.0). All calculations were performed on a MacBook Pro by using a M1 processor, Kernel Version Darwin 22.6.0 and macOS 13.5.2. All code is available under github.com/paulovic96.

Statistics

P values for comparison of 2 groups were calculated using unpaired 2-tailed Mann-Whitney *U* tests. *P* values are indicated as follows: $*P < .05$; $**P < .01$; $***P < .001$. In the principal component (PC) analyses (PCAs), Pillai-MANOVA was used as a statistical test. The ellipse in PCA plots refers to 3 times the euclidian distance. Raincloud plots were created by using Matplotlib 3.8.4, and statistical analyses were performed by using python 3.11.6 with scipy.stats 1.12.0 or statsmodels 0.14.0.

RESULTS

Clinical characteristics of the DADA2 cohort

We analyzed the samples of 52 patients with DADA2 who were seen at the NIH Clinical Center between 2014 and 2022. At presentation, a median age of 12 years (range 1-56 years; 60% female and 40% male). A detailed description of the study design is provided elsewhere.[19] Basic clinical, demographic, and genetic characteristics are summarized in Table I. The most common clinical manifestations were livedo racemosa (73% [in 38 of 52 patients]), fever (69% [in 36 of 52 patients]), and polyarteritis nodosa (PAN)/nodules (48% [in 25 of 52 patients]). Further common symptoms related to autoimmunity or vasculitis were antinuclear antibody positivity (27% [in 13 of 49 individuals tested]), Raynaud syndrome (25% [in 13 of 52 patients]), and lymphadenopathy (16% [in 8 of 51 patients with available data]) (Table I). From the sampled patients with DADA2, 24 (47%) had at least 1 stroke (Table I). Serologic manifestations included increased C-reactive protein levels in 77% of patients (40 of 52) and low immunoglobulin levels in 65% of patients (34 of 52) (Table I and Fig 1, *A*). Of all the hypogammaglobulinemic patients, 43% had reduced IgM levels, 33% had reduced IgG levels, and 32% had reduced IgA levels (Fig 1, *A*). Immunoglobulin serum titers positively correlated with each other (Fig 1, *B*). If not supplemented, the immunoglobulin titers persisted over time in most of the patients (Fig 1, *C*). In addition, 48% of the analyzed patients (25 of 52) displayed cytopenias (Table I and Fig 1, *D*). Flow cytometric lymphocyte profiling revealed normal counts for $CD4^+$ and $CD8^+$ T cells, as well as for $CD20^+$ B cells in most patients (Fig 1, *D*). However, the memory B-cell compartment ($CD20^+CD27^+$), as well as CD4 effector memory ($CD4^+CD62L^+CD45RA^+$) and CD4 central memory ($CD4^+CD62L^-CD45RA^-$) populations, were commonly contracted (Fig 1, *D*). In addition, the numbers of circulating $CD56^+$ natural killer cells were reduced in 40% of patients with DADA2 (Fig 1, *D*).

Cytokine dysregulation in patients with DADA2

Next, we quantified the levels of 21 soluble factors essential to B- and T-cell immune regulation in 18 patients with available serum samples. Serum samples from healthy individuals (n = 19) served as a control. We observed substantially elevated serum levels of the proinflammatory cytokines TNF and IL-8; the B-cell survival and proliferation factors a proliferation-inducing ligand (APRIL), B-cell activating factor (BAFF), and soluble CD40 ligand (sCD40L); and the type 1 IFN-β– and IFN-γ–responsive factor IP-10 (CXCL10) in line with IFN-associated T-cell transcriptome signatures in DADA2-derived T cells[24] (Fig 1, *E*). The mean levels of IFN-α2, IFN-γ, and IFN-λ1 also trended toward higher levels but did not achieve statistical significance (Fig 1, *E*). Although the levels of IL-8, APRIL and the interferons normalized under anti-TNF therapy, elevated serum levels of TNF, IP-10, BAFF, and sCD40L persisted (Fig 1, *E*). A correlation analysis of the detected serum levels revealed a strong positive correlation between BAFF, APRIL, sCD40L, IL-8, and IFN-α2 in untreated patients that, with the exception of BAFF and IL-8, resolved in TNF-treated patients (Fig 1, *F*). Although interferons generally appeared positively correlated, the clearest correlation patterns differed between treated and untreated patients (Fig 1, *F*). Untreated patients with DADA2 displayed strong positive correlations of IFN-β and IFN-λ2/3, whereas treated patients with DADA2 exhibited correlations between IFN-β and IFN-λ1 as well as between IFN-λ2/3 and IFN-α2 (Fig 1, *F*). Interestingly, the levels of TNF showed no positive correlation with any of the analyzed factors but were rather negatively correlated with IFN-γ, IFN-λ1, and IL-10 in untreated patients (Fig 1, *F*). Notably, we observed positive correlations between CD4 effector memory cell frequencies and IL-8 levels, as well as between nonmemory CD20 populations and IL-1β and IL-8 (see Fig E1 in the Online Repository at www.jaciconline.

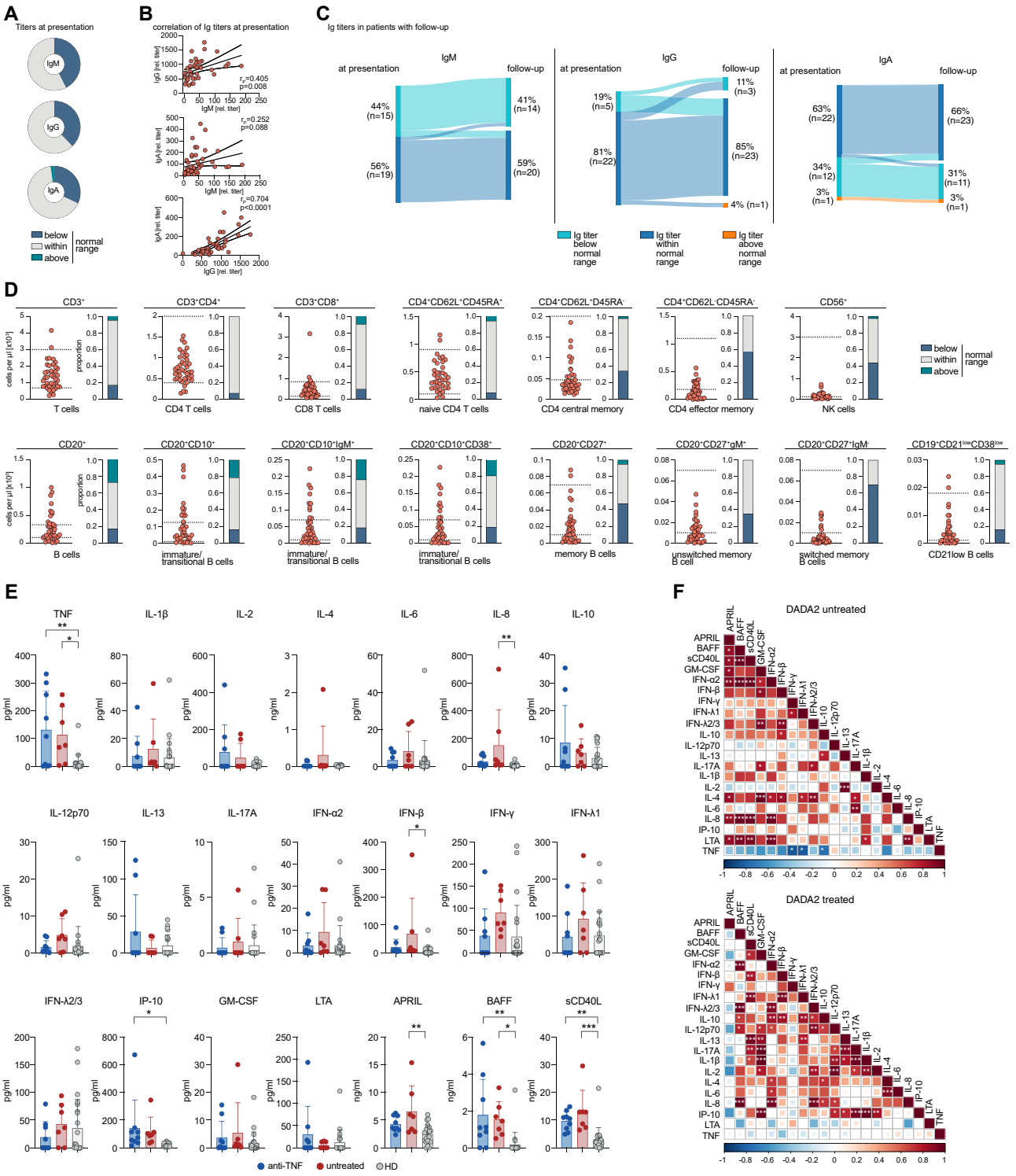

FIG 1. Immunologic features of the DADA2 cohort. **A,** Proportions of patients with DADA2 with increased, decreased, or normal titers of IgM (n = 47), IgG (n = 37), and IgA (n = 47) serum titers at presentation. **B,** Correlation of IgM, IgG, and IgA titers. Spearman correlation coefficients (r_S) and *P* values are indicated. **C,** Migration plot indicating change in Ig levels between first presentation and follow-up. **D,** Flow cytometric quantification of indicated peripheral B- and T-cell populations. Detected cell numbers per microliter as dot plots, with dotted lines indicating the normal range. Bar plot indicating the proportions of patients with DADA2 (n = 37-41) with increased, decreased, or normal cell counts. **E,** Quantification of indicated soluble factors and cytokines in the serum of patients with DADA2 (n = 18) and healthy donors (HD [n = 19]). Untreated patients with DADA2 (n = 7) and patients with DADA2 under anti-TNF (infliximab) therapy (n = 9). Bars indicate means ± SDs. Unpaired 2-sided *t* test; **P* < .05; ***P* < .01; ****P* < .001. **F,** Correlation matrix of soluble serum cytokines in patients with DADA2.

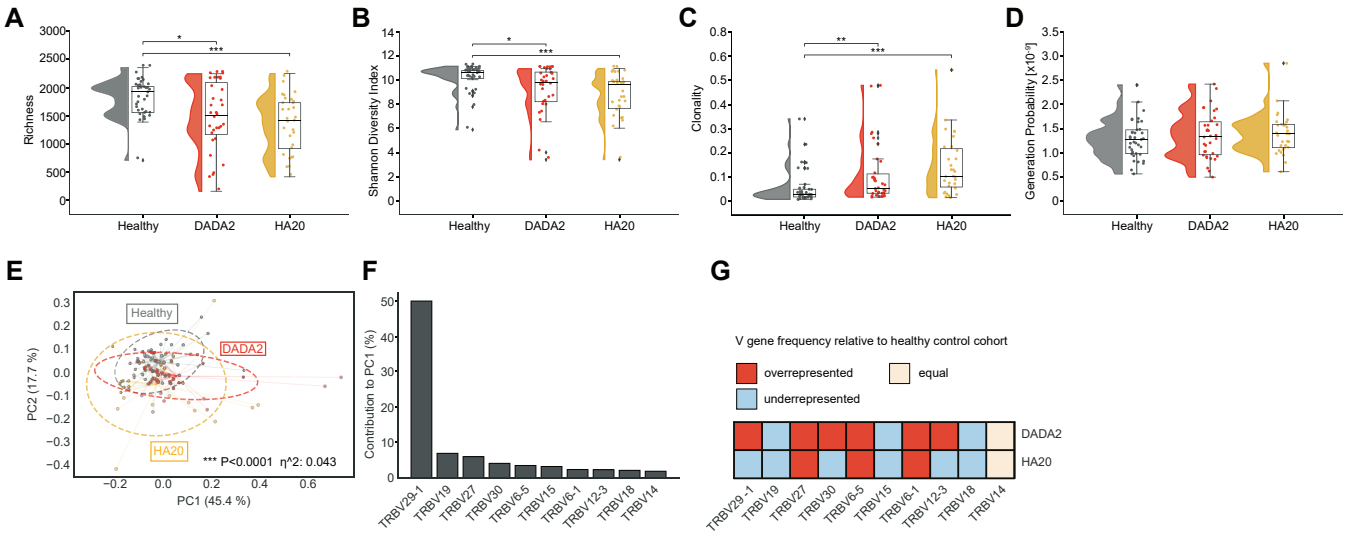

FIG 2. Blood T-cell repertoire metrics of the DADA2 cohort versus those of age-matched control individuals. **A-C,** Normalized TCR repertoire richness (**A**), diversity (**B**), and clonality (**C**) of patients with DADA2 (n = 34) versus control immune repertoires from age-matched healthy individuals (n = 37) and patients with HA20 (n = 31) as disease controls. Mann-Whitney *U* test; **P* < .05; ***P* < .01; ****P* < .001. **D,** Median generation probability per repertoire in the DADA2 versus control cohort. **E,** TCR V gene distribution as assessed by PCA. Statistics: Pillai-Bartlett test of multivariate ANOVA (MANOVA) of all PCs. **F,** V genes contributing most to the repertoire skewing on PC 1 . **G,** Mean frequency of V gene use from (**F**) in patients with DADA2 and patients with HA20 versus in healthy individuals.

org). IFN-λ2 and IFN-λ2/3 levels correlated with transitional B cells. TNF, BAFF, and APRIL levels showed trends of negative correlation with most lymphocyte subsets, although these did not reach statistical significance (see Fig E1).

Immunogenetic profiling of the DADA2 cohort and age-matched control individuals

To get further insights into DADA2 immune dysregulation, we determined the peripheral blood immune repertoire architecture of T and B cells in our patients with DADA2 by next-generation sequencing of the rearranged TRB and IGH loci. Because age has a fundamental impact on the adaptive immune architecture,[25-27] we compiled an age-matched control cohort of 45 healthy individuals with a median age of 15 years (range 1-55 years) and a female-to-male ratio of 53%:47% as an unbiased control,[28] As a disease control for a monogenetic autoinflammatory disease characterized by nuclear factor-κB (NF-κB) dysregulation and systemic TNF elevations, we used the immunogenetic data from a cohort of patients with haploinsufficiency of A20 (HA20).[29] TCR repertoires of patients with DADA2 showed reduced richness and diversity but higher clonality than those of their age-matched healthy peers (Fig 2, *A-C*). The HA20 TCR repertoires showed a similar architecture but were more pronounced than in the DADA2 setting with high clonality and reduced indices for diversity and richness (Fig 2, *A-C*). The median generation probability of TCR rearrangements as a measure of the frequency of public clonotypes was similar between the DADA2, HA20, and healthy control T-cell repertoires (Fig 2, *D*). PCA of the TRBV gene use showed considerable skewing of the DADA2 and HA20 T-cell repertoire as compared with that of the healthy controls (Fig 2, *E*). Although patterns of TRBV19, TRBV27, TRBV6-5, and TRBV6-1 use were shared between patients with DADA2 and patients with HA20 versus with healthy controls, DADA2 skewing was additionally driven by differential use of TRBV29-1 genes (Fig 2, *F* and *G*).

In contrast to the TCR repertoires, the BCR repertoires of patients with DADA2 displayed less clear differences in basic repertoire metrics such as richness, diversity, and clonality than their age-matched healthy controls did (Fig 3, *A-C*). In contrast, the HA20 BCR repertoires were characterized by reduced richness and diversity, as well as by higher clonality (Fig 3, *A-C*). As expected, the rate of somatic hypermutation of BCRs was substantially lower than that of the healthy controls and patients with HA20, reflecting the known lack of memory B cells in patients with DADA2 (Fig 3, *D*). PCA analysis also revealed a strongly biased IGHV gene distribution towards specific receptor rearrangements in patients with DADA2 (Fig 3, *E*). The BCR repertoires of patients with DADA2 were especially characterized by increased use of IGHV4-34, which has inherent autoreactive properties[30,31] (Fig 3, *F* and *G*). Notably, patients with DADA2 share this pattern with patients with HA20 (Fig 3, *F* and *G*).

Machine learning analysis of antigen receptor imprints

TCR and BCR repertoire data contain complex multilevel information on the immune architecture of an individual (or group of individuals) that can be extracted by developing machine learning tools with high predictive performance.[32,33] To identify a set of repertoire features that specifically defines DADA2 immunotypes by using machine learning, we trained a binary classifier to distinguish the T- and B-cell immune repertoires of patients with DADA2 from those of age-matched heathy controls. This resulted in a LightGBM classifier exhibiting the best performance among all tested models. The classifier showed robust performance, with an accuracy of 80% and an area under the curve of 0.88 on unseen data. The receiver operating characteristic curves

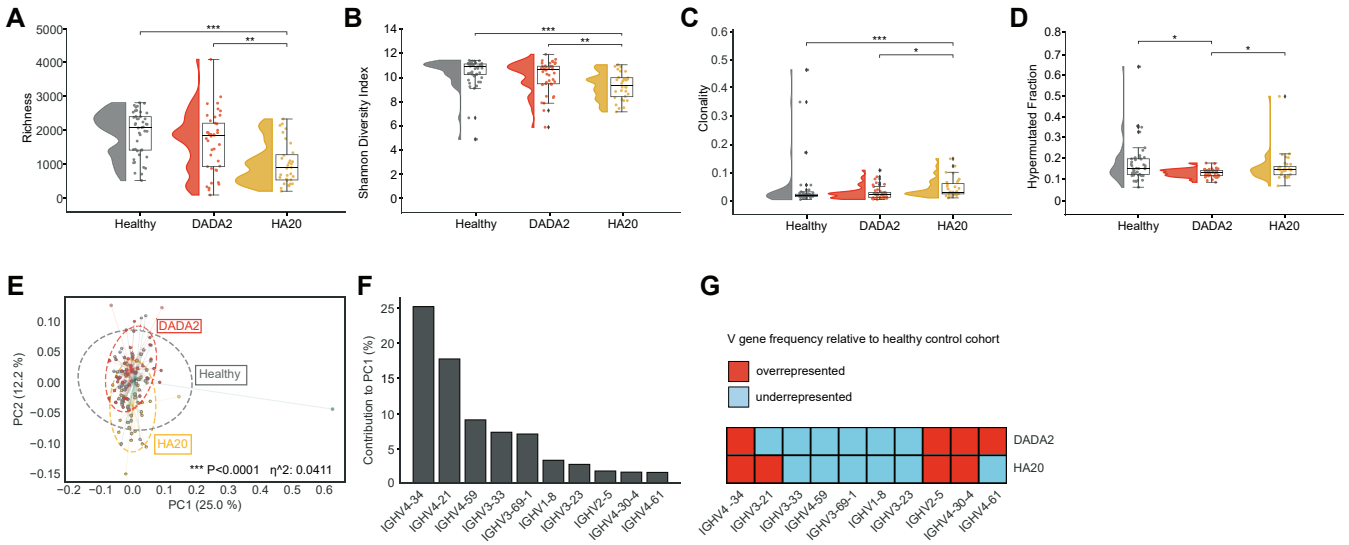

FIG 3. Blood B-cell repertoire metrics of the DADA2 cohort versus those of control individuals. **A-C,** Normalized BCR repertoire richness **(A)**, diversity **(B),** and clonality **(C)** of patients with DADA2 (n = 50) versus control immune repertoires from age-matched healthy individuals (n = 45) and patients as HA20 (n = 32) as a disease control. Statistics: Mann-Whitney *U* test; **P* < .05; ***P* < .01; ****P* < .001. **D,** Somatic hypermutation (SHM) of BCRs in the DADA2 cohort versus in control cohorts. **E,** PCA of BCR V gene use in the DADA2 cohort versus in age-matched healthy individuals and patients with HA20. Statistics: Pillai-Bartlett test of multivariate analysis of variance (MANOVA) of all PCs. **F,** V genes contributing most to the repertoire skewing on PC 1. **G,** Mean frequency of V gene use from (**F**) in patients with DADA2 and patients with HA20 versus in healthy individuals.

of the LightGBM classifier on the training, validation, and test samples are shown in Fig 4, *A*. A feature importance analysis revealed key features driving the classification of patients with DADA2 (Fig 4, *B* and *C*). The most important features for accurate classification of DADA2 were related to the B-cell space, mainly reduced B-cell richness and hypermutated B-cell fractions. Additionally, the model leveraged information regarding B-cell clone fraction; CDR3 length; and Kidera factors 2 (side chain size), 3 (extended structure preference), and 4 (hydrophobicity) of the CDR3 sequence of the most dominant clonotype within each repertoire. T-cell repertoire features also contributed to the classifier but were of relatively lesser importance. These included T-cell richness, V gene use (especially TRBV29-1 use of the dominant TCR clonotype), and length of CDR3. Importantly, there were no obvious correlations between the individual features of the model (see Fig E2 in the Online Repository at www.jaciconline.org). Fig 4, *D* and *E* show model performance in 2 exemplary cases. Taken together, the data show that our trained LightGBM classifier captured the autoimmune imprint of DADA2 immune repertoires with high fidelity, with a high feature importance for B-cell repertoire metrics.

DISCUSSION

The intersection of immunodeficiency and inflammation presents a complex challenge in many inherited immunologic disorders, such as DADA2, in which patients exhibit hypogammaglobulinemia and impaired T- and B-cell functionality alongside autoinflammation and autoimmune-mediated organ damage.[4,34-37] Besides, chronic dysregulation in adaptive cells may predispose patients with primary immunodeficiencies to develop lymphomas.[38] Our investigation of the adaptive immune architecture of patients with DADA2 in combination with soluble blood-circulating factors sheds light on the aberrant immunologic subpopulations present in DADA2 that warrant discussion and consideration for clinical management.

One of this study's key findings was the machine learning–based identification of patients with DADA2 using immunogenetic repertoire data. Our machine learning approach identified reduced richness and diversity metrics, as well as considerable skewing of TCR and BCR repertoires as major determinants of DADA2 immunotypes with high predictive value. The observed skewing was dominated by increased use of TRBV29-1–encoded TCR rearrangements, which are often found on autoreactive T cells[39,40] and by an enrichment of IGHV4-34–encoded antigen receptor configurations in B cells, which are known for their inherent autoreactive properties.[30,41-43] In addition, the predictive value of reduced somatic hypermutation is in line with the observation that autoimmune flares or *de novo* autoreactivity, especially in the context of IGHV4-34–encoded BCRs, are often characterized by activated naive cells.[44,45] The observed repertoire restriction is consistent with the immunosuppressive phenotype of patients with DADA2, whereas the immunogenetic shifts suggest a clinically relevant predisposition to autoimmunity. Importantly, the high accuracy of our trained LightGBM classifier in identifying patients with DADA2 on the basis of immune repertoire metric data alone, but not sequence-level labels, highlights the unique immunogenetic architecture in DADA2 and particularly emphasizes B-cell repertoire biases. Elevated levels of inflammatory cytokines, notably, TNF, BAFF (TNF superfamily member 13b), and interferons, likely contribute to these autoimmune-like imprints. This is supported by recent finding that the TNF/NF-κB signaling axis can shape immune repertoires by selectively driving the polyclonal expansion of

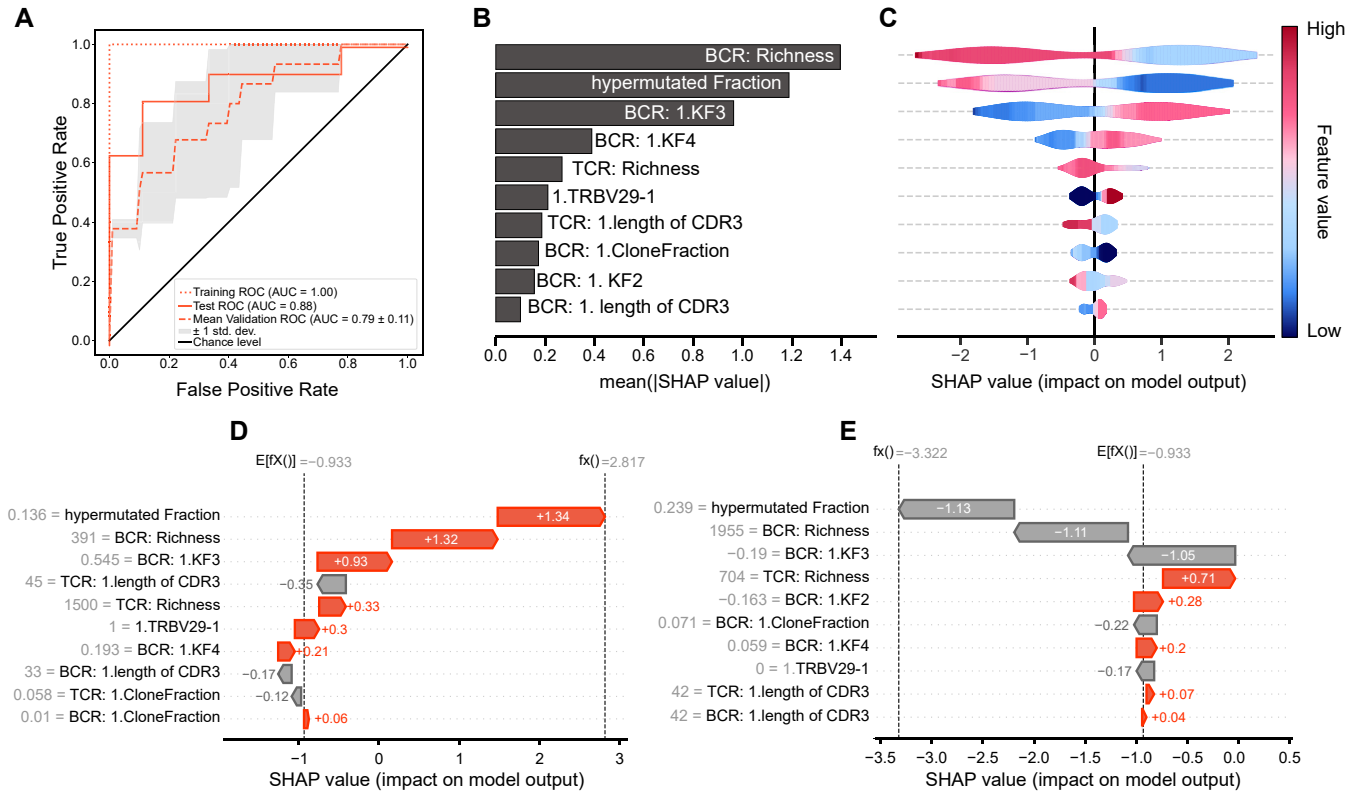

FIG 4. Machine learning classifier of autoimmune imprint in adaptive immune repertoires of patients with DADA2. **A,** Receiver operating characteristic (ROC) curve of lightGBM classifier on training, validation, and test samples. Curves demonstrate the classification performance of the trained classifier for distinguishing DADA2 from healthy immune profiles as a trade-off between true positive rate (sensitivity) and false-positive rate (1 – specificity). Area under the curve of 0.85 showed superior discriminatory ability of the trained model in identifying cases of DADA2 compared with the chance level. **B,** Variable importance analysis of a LightGBM classifier using Shapley Additive exPlanation (SHAP) values. Importance of the top 10 global features determined by mean absolute magnitude of SHAP value across all training samples. Values represent absolute changes in log odds, with higher values indicating greater feature importance. **C,** Distribution of SHAP values across training samples along with their corresponding feature value. Whereas positive SHAP values indicate that the feature contributes to raising the predicted probability of the positive class (DADA2), negative values suggest the opposite effect. **D,** Impact of individual features predicting a positive class (DADA2) test sample, showcasing how each feature contributes to shifting the model from its baseline prediction. Positive values indicating a higher likelihood of predicting the positive class, whereas negative values indicate a lower tendency to predict the positive class. **E,** Similarly, individual features have an impact on predicting a negative class (healthy donor [HD]) test sample.

IGHV4-34–encoded BCRs in patients with HA20,[29] a pattern that we also observed in patients with DADA2 and systemic TNF elevations that persisted under therapy, although this latter observation needs to be validated in additional patients. The high TNF levels originate mostly from proinflammatory polarization of macrophages driven by the loss or reduction of ADA2 function.[46] Interestingly, BCR repertoires can normalize under anti-TNF treatment in HA20.[29] These data align with the notion that NF-κB dysregulation is a shared molecular driver of HA20 and DADA2 pathology,[47,48] and they are consistent with the observation that TNF inhibitors are highly effective in reducing HA20 symptoms and suppressing inflammation in patients with DADA2.[29,37,48,49] The persistence of TNF elevations under therapy also aligns with the recurrence of disease flares after suboptimal dosing or discontinuation of anti-TNF therapy.[37]

In the context of stroke, the detected serum levels of sCD40L are noteworthy. The soluble form of CD40L (sCD154) is shed mainly from activated T cells and associated with platelet activation and aggregation, and it serves as marker for cardiovascular disease, carotid atherosclerosis, and recurrent stroke.[50-53] The observation of persisting sCD40L elevation under anti-TNF therapy may indicate a contributing role in mediating vascular inflammation, thrombosis, and recurrent strokes in patients with DADA2. Nevertheless, this aspect needs further investigation, especially with respect to the observation that anti-TNF therapy prevents ischemic and hemorrhagic strokes in patients with DADA2.[19,37]

Despite a few reported lymphoma cases in patients with DADA2, the risk of lymphoma potentially associated with the DADA2 genotype remains unclear.[54-58] Yet, the clonal expansion of immune cells bearing autoreactive antigen receptors such as

IGHV4-34, which is preferentially used in diffuse-large B-cell lymphoma, raises concerns regarding the transformation potential of these cells.[29,59] This is also supported by the association of *ADA2* variants with certain lymphoid malignancies.[60] At the same time, the requirement of TNF and BAFF signaling for survival of malignant lymphocytes in the tumor microenvironment[61-64] may equally be a mechanism sustaining survival of premalignant lymphocyte stages in the DADA2 setting. TNF blockade, therefore, not only emerges as a promising strategy to reverse autoimmunity but may also mitigate lymphoma risk in patients with DADA2. Along this line of reasoning, machine learning holds promise as a tool for unbiased detection of pathologic repertoire patterns and longitudinal monitoring of immune dynamics, offering insights into disease progression and treatment response.

Moving forward, further research is warranted to elucidate the drivers of autoimmune imprinting in DADA2 and explore the efficacy of targeted interventions, including TNF blockade, in mitigating autoimmunity and lymphoma risk. Longitudinal studies leveraging machine learning approaches can provide valuable insights into the evolving immune landscape of patients with DADA2, guiding personalized therapeutic strategies and improving clinical outcomes.

DISCLOSURE STATEMENT

Supported by the German Research Foundation (award SFB 1648/1 2024–512741711 [to M.B.]), the Swiss National Science Foundation (award 10.001.762 [to M.B.]), and the Mertelsmann Foundation (project grant to M.B.).

Disclosure of potential conflict of interest: The authors declare that they have no relevant conflicts of interest.

We thank the families of our DADA2 cohort for their great support. Moreover, we thank Christoph Wosiek and Aline Patzschke for excellent technical assistance. We are grateful to the Collaborative Research Institute Intelligent Oncology (CRIION), which supported the machine learning analyses performed in the context of this work.

Key messages

- **DADA2 is an autoinflammatory disease with a broad range of immune-related clinical features.**
- **Immunogenetic analyses of T and B cells reveal a unique immune architecture that not only reflects autoimmunity but also displays lymphoma-like imprints.**

REFERENCES

1. Di Virgilio F, Sarti AC, Falzoni S, De Marchi E, Adinolfi E. Extracellular ATP and P2 purinergic signalling in the tumour microenvironment. Nat Rev Cancer 2018;18:601-18.
2. Cekic C, Linden J. Purinergic regulation of the immune system. Nat Rev Immunol 2016;16:177-92.
3. Huang Z, Xie N, Illes P, Di Virgilio F, Ulrich H, Semyanov A, et al. From purines to purinergic signalling: molecular functions and human diseases. Signal Transduct Target Ther 2021;6:162.
4. Lee PY, Aksentijevich I, Zhou Q. Mechanisms of vascular inflammation in deficiency of adenosine deaminase 2 (DADA2). Semin Immunopathol 2022;44:269-80.
5. Zavialov AV, Engstrom A. Human ADA2 belongs to a new family of growth factors with adenosine deaminase activity. Biochem J 2005;391(Pt 1):51-7.
6. Greiner-Tollersrud OK, Krausz M, Boehler V, Polyzou A, Seidl M, Spahiu A, et al. ADA2 is a lysosomal deoxyadenosine deaminase acting on DNA involved in regulating TLR9-mediated immune sensing of DNA. Cell Rep 2024;43:114899.
7. Zhou Q, Yang D, Ombrello AK, Zavialov AV, Toro C, Zavialov AV, et al. Early-onset stroke and vasculopathy associated with mutations in ADA2. N Engl J Med 2014;370:911-20.
8. Navon Elkan P, Pierce SB, Segel R, Walsh T, Barash J, Padeh S, et al. Mutant adenosine deaminase 2 in a polyarteritis nodosa vasculopathy. N Engl J Med 2014;370:921-31.
9. Pinto B, Deo P, Sharma S, Syal A, Sharma A. Expanding spectrum of DADA2: a review of phenotypes, genetics, pathogenesis and treatment. Clin Rheumatol 2021;40:3883-96.
10. Moens L, Hershfield M, Arts K, Aksentijevich I, Meyts I. Human adenosine deaminase 2 deficiency: a multi-faceted inborn error of immunity. Immunol Rev 2019;287:62-72.
11. Lee PY, Kellner ES, Huang Y, Furutani E, Huang Z, Bainter W, et al. Genotype and functional correlates of disease phenotype in deficiency of adenosine deaminase 2 (DADA2). J Allergy Clin Immunol 2020;145:1664-72.e10.
12. Bulte D, Barzaghi F, Mesa-Nunez C, Rigamonti C, Basso-Ricci L, Visconti C, et al. Early bone marrow alterations in patients with adenosine deaminase 2 deficiency across disease phenotypes and severities. J Allergy Clin Immunol 20241155:616-27.e8.
13. Schepp J, Proietti M, Frede N, Buchta M, Hubscher K, Rojas Restrepo J, et al. Screening of 181 patients with antibody deficiency for deficiency of adenosine deaminase 2 sheds new light on the disease in adulthood. Arthritis Rheumatol 2017;69:1689-700.
14. Schena F, Penco F, Volpi S, Pastorino C, Caorsi R, Kalli F, et al. Dysregulation in B-cell responses and T follicular helper cell function in ADA2 deficiency patients. Eur J Immunol 2021;51:206-19.
15. Yap JY, Moens L, Lin MW, Kane A, Kelleher A, Toong C, et al. Intrinsic defects in B cell development and differentiation, T cell exhaustion and altered unconventional T cell generation characterize human adenosine deaminase type 2 deficiency. J Clin Immunol 2021;41:1915-35.
16. Schepp J, Bulashevska A, Mannhardt-Laakmann W, Cao H, Yang F, Seidl M, et al. Deficiency of adenosine deaminase 2 causes antibody deficiency. J Clin Immunol 2016;36:179-86.
17. Skrabl-Baumgartner A, Plecko B, Schmidt WM, Konig N, Hershfield M, Gruber-Sedlmayr U, et al. Autoimmune phenotype with type I interferon signature in two brothers with ADA2 deficiency carrying a novel CECR1 mutation. Pediatr Rheumatol Online J 2017;15:67.
18. Maccora I, Maniscalco V, Campani S, Carrera S, Abbati G, Marrani E, et al. A wide spectrum of phenotype of deficiency of deaminase 2 (DADA2): a systematic literature review. Orphanet J Rare Dis 2023;18:117.
19. Barron KS, Aksentijevich I, Deuitch NT, Stone DL, Hoffmann P, Videgar-Laird R, et al. The spectrum of the deficiency of adenosine deaminase 2: an observational analysis of a 60 patient cohort. Front Immunol 2021;12:811473.
20. Schultheiss C, Simnica D, Willscher E, Oberle A, Fanchi L, Bonzanni N, et al. Next-generation immunosequencing reveals pathological T-cell architecture in autoimmune hepatitis. Hepatology 2021;73:1436-48.
21. Simnica D, Schliffke S, Schultheiss C, Bonzanni N, Fanchi LF, Akyuz N, et al. High-throughput immunogenetics reveals a lack of physiological T cell clusters in patients with autoimmune cytopenias. Front Immunol 2019;10:1897.
22. Bolotin DA, Poslavsky S, Mitrophanov I, Shugay M, Mamedov IZ, Putintseva EV, et al. MiXCR: software for comprehensive adaptive immunity profiling. Nat Methods 2015;12:380-1.
23. Sethna Z, Elhanati Y, Callan CG, Walczak AM, Mora T. OLGA: fast computation of generation probabilities of B- and T-cell receptor amino acid sequences and motifs. Bioinformatics 2019;35:2974-81.
24. Wu Z, Gao S, Watanabe N, Batchu S, Kajigaya S, Diamond C, et al. Single-cell profiling of T lymphocytes in deficiency of adenosine deaminase 2. J Leukoc Biol 2022;111:301-12.
25. Simnica D, Akyuz N, Schliffke S, Mohme M, L VW, Mahrle T, et al. T cell receptor next-generation sequencing reveals cancer-associated repertoire metrics and reconstitution after chemotherapy in patients with hematological and solid tumors. Oncoimmunology 2019;8:e1644110.
26. Paschold L, Simnica D, Willscher E, Vehreschild MJ, Dutzmann J, Sedding DG, et al. SARS-CoV-2-specific antibody rearrangements in prepandemic immune repertoires of risk cohorts and patients with COVID-19. J Clin Invest 2021;131:e142966.
27. Simnica D, Schultheiss C, Mohme M, Paschold L, Willscher E, Fitzek A, et al. Landscape of T-cell repertoires with public COVID-19-associated T-cell receptors in pre-pandemic risk cohorts. Clin Transl Immunology 2021;10:e1340.

28. Paschold L, Gottschick C, Langer S, Klee B, Diexer S, Aksentijevich I, et al. T cell repertoire breadth is associated with the number of acute respiratory infections in the LoewenKIDS birth cohort. Sci Rep 2023;13:9516.
29. Schultheiss C, Paschold L, Mohebiany AN, Escher M, Kattimani YM, Muller M, et al. A20 haploinsufficiency disturbs immune homeostasis and drives the transformation of lymphocytes with permissive antigen receptors. Sci Adv 2024;10:eadl3975.
30. Pugh-Bernard AE, Silverman GJ, Cappione AJ, Villano ME, Ryan DH, Insel RA, et al. Regulation of inherently autoreactive VH4-34 B cells in the maintenance of human B cell tolerance. J Clin Invest 2001;108:1061-70.
31. Fujio K, Ushijima T, Okamura T, Ota M. The role of polyreactive memory B cells in systemic lupus erythematosus [e-pub ahead of print]. Int Immunol https://doi.org/10.1093/intimm/dxae058. Accessed November 8, 2024.
32. Vu MH, Robert PA, Akbar R, Swiatczak B, Sandve GK, Haug DTT, et al. Linguistics-based formalization of the antibody language as a basis for antibody language models. Nat Comput Sci 2024;4:412-22.
33. Schmidt-Barbo P, Kalweit G, Naouar M, Paschold L, Willscher E, Schultheiss C, et al. Detection of disease-specific signatures in B cell repertoires of lymphomas using machine learning. PLoS Comput Biol 2024;20:e1011570.
34. Dzhus M, Ehlers L, Wouters M, Jansen K, Schrijvers R, De Somer L, et al. A Narrative review of the neurological manifestations of human adenosine deaminase 2 deficiency. J Clin Immunol 2023;43:1916-26.
35. Wouters M, Ehlers L, Dzhus M, Kienapfel V, Bucciol G, Delafontaine S, et al. Human ADA2 deficiency: ten years later. Curr Allergy Asthma Rep 2024;24:477-84.
36. Grim A, Veiga KR, Saad N. Deficiency of adenosine deaminase 2: clinical manifestations, diagnosis, and treatment. Rheum Dis Clin North Am 2023;49:773-87.
37. Lee PY, Davidson BA, Abraham RS, Alter B, Arostegui JI, Bell K, et al. Evaluation and management of deficiency of adenosine deaminase 2: an international consensus statement. JAMA Netw Open 2023;6:e2315894.
38. Bousfiha A, Moundir A, Tangye SG, Picard C, Jeddane L, Al-Herz W, et al. The 2022 update of IUIS phenotypical classification for human inborn errors of immunity. J Clin Immunol 2022;42:1508-20.
39. Eugster A, Lorenc A, Kotrulev M, Kamra Y, Goel M, Steinberg-Bains K, et al. Physiological and pathogenic T cell autoreactivity converge in type 1 diabetes. Nat Commun 2024;15:9204.
40. Ciacchi L, Farenc C, Dahal-Koirala S, Petersen J, Sollid LM, Reid HH, et al. Structural basis of T cell receptor specificity and cross-reactivity of two HLA-DQ2.5-restricted gluten epitopes in celiac disease. J Biol Chem 2022;298:101619.
41. Schickel JN, Glauzy S, Ng YS, Chamberlain N, Massad C, Isnardi I, et al. Self-reactive VH4-34-expressing IgG B cells recognize commensal bacteria. J Exp Med 2017;214:1991-2003.
42. Richardson C, Chida AS, Adlowitz D, Silver L, Fox E, Jenks SA, et al. Molecular basis of 9G4 B cell autoreactivity in human systemic lupus erythematosus. J Immunol 2013;191:4926-39.
43. Cappione AJ, Pugh-Bernard AE, Anolik JH, Sanz I. Lupus IgG VH4.34 antibodies bind to a 220-kDa glycoform of CD45/B220 on the surface of human B lymphocytes. J Immunol 2004;172:4298-307.
44. Tipton CM, Fucile CF, Darce J, Chida A, Ichikawa T, Gregoretti I, et al. Diversity, cellular origin and autoreactivity of antibody-secreting cell population expansions in acute systemic lupus erythematosus. Nat Immunol 2015;16:755-65.
45. Woodruff MC, Ramonell RP, Haddad NS, Anam FA, Rudolph ME, Walker TA, et al. Dysregulated naive B cells and de novo autoreactivity in severe COVID-19. Nature 2022;611:139-47.
46. Zoccolillo M, Brigida I, Barzaghi F, Scala S, Hernandez RJ, Basso-Ricci L, et al. Lentiviral correction of enzymatic activity restrains macrophage inflammation in adenosine deaminase 2 deficiency. Blood Adv 2021;5:3174-87.
47. Zhou Q, Wang H, Schwartz DM, Stoffels M, Park YH, Zhang Y, et al. Loss-of-function mutations in TNFAIP3 leading to A20 haploinsufficiency cause an early-onset autoinflammatory disease. Nat Genet 2016;48:67-73.
48. Nigrovic PA, Lee PY, Hoffman HM. Monogenic autoinflammatory disorders: conceptual overview, phenotype, and clinical approach. J Allergy Clin Immunol 2020;146:925-37.
49. Karri U, Harasimowicz M, Carpio Tumba M, Schwartz DM. The complexity of being A20: from biological functions to genetic associations. J Clin Immunol 2024;44:76.
50. Tang T, Cheng X, Truong B, Sun L, Yang X, Wang H. Molecular basis and therapeutic implications of CD40/CD40L immune checkpoint. Pharmacol Ther 2021;219:107709.
51. Wagner AH, Klersy A, Sultan CS, Hecker M. Potential role of soluble CD40 receptor in chronic inflammatory diseases. Biochem Pharmacol 2023;217:115858.
52. Shami A, Edsfeldt A, Bengtsson E, Nilsson J, Shore AC, Natali A, et al. Soluble CD40 levels in plasma are associated with cardiovascular disease and in carotid plaques with a vulnerable phenotype. J Stroke 2021;23:367-76.
53. Li J, Wang Y, Lin J, Wang D, Wang A, Zhao X, et al. Soluble CD40L is a useful marker to predict future strokes in patients with minor stroke and transient ischemic attack. Stroke 2015;46:1990-2.
54. Springer JM, Gierer SA, Jiang H, Kleiner D, Deuitch N, Ombrello AK, et al. Deficiency of adenosine deaminase 2 in adult siblings: many years of a misdiagnosed disease with severe consequences. Front Immunol 2018;9:1361.
55. Alabbas F, Elyamany G, Alsharif O, Hershfield M, Meyts I. Childhood Hodgkin lymphoma: think DADA2. J Clin Immunol 2019;39:26-9.
56. Andriessen MVE, Legger GE, Bredius RGM, van Gijn ME, Hak AE, Muller P, et al. Clinical symptoms, laboratory parameters and long-term follow-up in a national DADA2 cohort. J Clin Immunol 2023;43:1581-96.
57. Albalawi R, Hanafy E, Alnafea H, Altowijiry M, Riyad S, Abufara F, et al. Novel adenosine deaminase 2 (ADA2) mutations associated with hematological manifestations. J Investig Med High Impact Case Rep 2021;9:2324709621105 6770.
58. Manhal A, Qouqas MM, Fasfoos A, Abdullah J, Abudaowd S, Amro O, et al. Deficiency of adenosine deaminase 2 leading to recurrent Hodgkin lymphoma: a case report., 12. SAGE Open Med Case Rep2050313X241260148.
59. Young RM, Wu T, Schmitz R, Dawood M, Xiao W, Phelan JD, et al. Survival of human lymphoma cells requires B-cell receptor engagement by self-antigens. Proc Natl Acad Sci U S A 2015;112:13447-54.
60. Cerami E, Gao J, Dogrusoz U, Gross BE, Sumer SO, Aksoy BA, et al. The cBio cancer genomics portal: an open platform for exploring multidimensional cancer genomics data. Cancer Discov 2012;2:401-4.
61. Nishio M, Endo T, Tsukada N, Ohata J, Kitada S, Reed JC, et al. Nurselike cells express BAFF and APRIL, which can promote survival of chronic lymphocytic leukemia cells via a paracrine pathway distinct from that of SDF-1alpha. Blood 2005;106:1012-20.
62. Lwin T, Crespo LA, Wu A, Dessureault S, Shu HB, Moscinski LC, et al. Lymphoma cell adhesion-induced expression of B cell-activating factor of the TNF family in bone marrow stromal cells protects non-Hodgkin's B lymphoma cells from apoptosis. Leukemia 2009;23:170-7.
63. Alim LF, Keane C, Souza-Fonseca-Guimaraes F. Molecular mechanisms of tumour necrosis factor signalling via TNF receptor 1 and TNF receptor 2 in the tumour microenvironment. Curr Opin Immunol 2024;86:102409.
64. Zhou X, Li Z, Zhou J. Tumor necrosis factor alpha in the onset and progression of leukemia. Exp Hematol 2017;45:17-26.